Cancer Res Treat. 2010;42(2):82-94 DOI 10.4143/crt.2010.42.2.82

Time-course Transcriptional Profiling of Human Amniotic Fluid-derived Stem Cells Using Microarray

Yong Wook Kim, M.D.[1]
Hyun-Jung Kim, Ph.D.[2]
Su-Mi Bae, Ph.D.[2]
Young Jae Kim, M.D.[3]
Jong-Chul Shin, M.D.[1]
Heung-Jae Chun, Ph.D.[4]
Jong-Won Rhie, Ph.D.[5]
Jiyoung Kim, Ph.D.[6]
Haekwon Kim, Ph.D.[6]
Woong Shick Ahn, M.D., Ph.D.[1,2]

[1]Department of Obstetrics and Gynecology, [2]Catholic Research Institutes of Medical Science, The Catholic University of Korea Colleg of Medicine, [3]Department of Obstetrics and Gynecology, College of Medicine, Hanyang University, Departments of [4]Biomedical Science, [5]Plastic Surgery, College of Medicine, The Catholic University of Korea, [6]Department of Biotechnology, Seoul Women's University College of Medicine, Seoul, Korea

Correspondence: Woong Shick Ahn, M.D., Ph.D.
Department of Obstetrics and Gynecology, College of Medicine, The Catholic University of Korea College of Medicine, 505, Banpo-dong, Seocho-gu, Seoul 137-040, Korea
Tel: 82-2-2258-6946
Fax: 82-2-599-4120
E-mail: ahnws@catholic.ac.kr
Received Marh 11, 2009
Accepted November 9, 2009

The authors wishes to acknowledge the financial support of the Catholic Medical Center Research Foundation made in the program year of 2007.

Purpose
To maintain the homeostasis of stem cells and prevent their ability to initiate tumorigenesis, it is important to identify and modify factors that prevent or accelerate stem cell senescence. We used microarrays to attempt to identify such factors in human amniotic fluid (HAF)-derived stem cells.

Materials and Methods
To identify gene expression changes over a time course, we compared gene expression profiles of HAF-derived stem cells in different passages (1st, 2nd, 4th, 6th, 8th, and 10th) using a Sentrix Human illumina microarray.

Results
Of the 25,804 genes in the microarray chip, 1,970 showed an over 2-fold change relative to the control (the 1st passage)-either upregulated or downregulated. Quantitative real-time PCR validated the microarray data for selected genes: markedly increased genes were CXCL12, cadherin 6 (CDH6), and folate receptor 3 (FOLR3). Downregulated genes included cyclin D2, keratin 8, insulin-like growth factor 2 (IGF2), natriuretic peptide precursor B (NPPB) and cellular retinoic acid binding protein 2 (CRABP2). The expression pattern of the selected genes was consistent with the microarray data except for CXCL12 and IGF2. Interestingly, the expression of NPPB was dramatically downregulated along the time course; it was almost completely shut-down by the 10th passage. In contrast, FOLR3 mRNA expression was dramatically increased.

Conclusion
Taken together, although a function for NPPB and FOLR3 in stem cell senescence has not been reported, our results strongly suggest that NPPB and/or FOLR3 play a significant role in the regulation of stem cell senescence.

Key words
Human amniotic fluid, Stem cells, Natriuretic peptide precursor B (NPPB), Folate receptor 3 (FOLR3)

Introduction

Although cells are routinely used for prenatal diagnosis of a wide range of foetal abnormalities caused by genetic defects, cell types present in human amniotic fluid (HAF) have not been thoroughly characterized. HAF obtained during amniocentesis includes a variety of stem cells originating from embryonic and extra-embryonic tissues (1), and cells of different embryonic/fetal origins of all three germ layers have been reported to exist in amniotic fluid (2). HAF has also been shown to contain cells expressing Oct-4 antigen, a specific marker of pluripotent stem cells (3), and these cells display multilineage differentiation potential; depending on the specific culture conditions, they can differentiate into adipocytes, osteocytes or neuronal cells (4). Thus, HAF is a possible source of pluripotent stem cells for cell-based therapeutics, a strategy that will not raise ethical concerns associated with use of embryonic stem cells (ESCs).

Cellular senescence might also contribute to a decline in tissue homeostasis by exhausting the supply of progenitor cells or stem cells due to irreversible growth arrest. The regulation of stem cell senescence has potential importance in different therapeutic strategies: one is cell therapy; the other is inhibition of expansion of the cancer stem cell population. For cell therapies such as cell transplantation in regenerative medicine, stem cell senescence must be prevented in order to acquire enough cells to achieve differentiation into specialized cell types. Conversely, for cancer therapy, stem cell senescence must be induced to prevent the proliferation and differentiation of transformed cancer stem cells.

Cellular senescence is usually accompanied by changes in gene expression. Normal mouse embryonic fibroblasts (MEFs) reach replicative senescence after seven passages in culture, whereas MEFs from Bmi-1$^{-/-}$ mice show a premature-senescence phenotype at the third passage (5), indicating the important role of Bmi-1 as a repressor of senescence. In flies, expression of a dominant-negative p53 extends life-span (6). Conversely, mice with activated p53 display signs of premature aging (7). Also, p21 (Waf1/Cip1/Sdi1), a downstream target of p53, is a powerful broad spectrum cyclin-dependent kinase (CDK) inhibitor that blocks the activity of cyclin-CDK2 and cyclin-CDK4/6 complexes that are required for cell cycle progression. An increase in p21 is a central feature of senescence (8). The other major effector of cell cycle arrest in human senescent cells is p16 (Ink4a). p16 inhibits cyclin D1-CDK4/6, which is the kinase complex responsible for pRb phosphorylation. p16 siRNA knockdown studies indicate that p16 is needed to maintain senescence in human fibroblasts (9).

In the current study, we examined gene expression profiles of HAF cells during senescence to identify new cellular senescence-associated genes, genes that might serve as targets for cancer therapy or cell therapy.

Materials and Methods

1 Human amniotic fluid (HAF) cell isolation and culture

HAF samples (5 mL each) were obtained from patients undergoing amniocentesis for routine prenatal diagnosis at 14～16 weeks of pregnancy. Cells were isolated from HAF no more than 12 h prior to use in experiments. HAF samples were centrifuged at 300×g for 15 min, and the resulting pellets were washed twice with low-glucose

Table 1. RT-qPCR primer sequences

Gene	Primer sequence	Accession number	Size (bp)	Annealing temp (C)
IGF2	For: 5'-CCTCCAGTTCGTCTGTGGG-3'	NM_000876	163 bp	60 C
	Rev: 5'-CACGTCCCTCTCGGACTTG-3'			
CDH6	For: 5'-ACCCAGTTCAAAGCAGCACT-3'	NM_004932	178 bp	60 C
	Rev: 5'-GCAAACAGCACCACTGTCAC-3'			
CRABP2	For: 5'-TCGGAAAACTTCGAGGAATTGC-3'	NM_001878	103 bp	60 C
	Rev: 5'-CCTGTTTGATCTCCACTGCTG-3'			
CXCL12	For: 5'-AGAGCCAACGTCAAGCATCT-3'	NM_199168.2	168 bp	60 C
	Rev: 5'-CCTTTTTGGCTGTTGTGCTT-3'			
CyclinD2	For: 5'-TGTGCCACCGACTTTAAGTTT-3'	NM_001759.2	172 bp	60 C
	Rev: 5'-CTTTGAGACAATCCACGTCTGT-3'			
KRT8	For: 5'-ACCCTCAACAACAAGTTTGCCTCC-3'	NM_002273.2	82 bp	60 C
	Rev: 5'-TCCACTTGGTCTCCAGCATCTTGT-3'			
NPPB	For: 5'-TCCTGCTCTTCTTGCATCTGGCTT-3'	NM_002521	112 bp	60 C
	Rev: 5'-AAATGGTTGCGCTGCTCCTGTAAC-3'			
FOLR3	For: 5'-TCAATGTCTGCATGAACGCCAAGC-3'	NM_000804	153 bp	60 C
	Rev: 5'-TAAAGTTGTACAGGCGGGAGGTGT-3'			
GAPDH	For: 5'-TTCGACAGTCAGCCGCATCTTCTT-3'	NM_002046	105 bp	60 C
	Rev: 5'-GCCCAATACGACCAAATCCGTTGA-3'			

Dulbecco's modified Eagle's medium (DMEM) (Invitrogen, Carlsbad, CA) to remove blood and cell debris. All cells isolated from the 5 mL sample were plated in a 35 cm^2 culture flask (Nunc, Rochester, MN) containing DMEM supplemented with 100 U/mL penicillin, 0.1 mg/mL streptomycin (Invitrogen), 3.7 mg/mL sodium bicarbonate, 10 ng/mL epidermal growth factor (EGF) (Peprotech, Princeton, NJ) and 10% foetal bovine serum (FBS) (Invitrogen). Seven days after the initiation of the culture, the medium was replaced with fresh medium, and subsequently was replaced twice a week. When the cells reached confluence, they were treated with 0.125% trypsin and 1 mM ethylenediamine tetraacetic acid (EDTA) for 3 min. The released cells were collected and replated for subculture. These HAF-derived fibroblastoid-type cells were maintained in a humidified atmosphere in an incubator under 5% CO_2 at 37℃.

2 RNA Isolation and Amplification for illumina microarray

Total RNA was extracted using Trizol® (Invitrogen) according to the manufacturer's protocol. After DNase digestion and clean-up procedures, RNA samples were quantified, aliquoted and stored at −80℃ until use. For quality control, RNA purity and integrity were evaluated by denaturing gel electrophoresis, OD 260/280 ratio, and analysis on an Agilent 2100 Bioanalyzer (Agilent Technologies, Palo Alto, CA).

Total RNA was amplified and purified using Ambion Illumina® RNA amplification kits (Ambion, Austin, TX) to yield biotinylated cRNA according to the manufacturer's instructions. Briefly, 550 ng of total RNA was reverse-transcribed to cDNA using a T7 oligo (dT) primer. Second-strand cDNA was synthesized, *in vitro* transcribed, and labeled with biotin-NTP. After purification, the cRNA was quantified using an ND-1000 Spectrophotometer (NanoDrop, Wilmington, DE).

3 Illumina microarray

The labeled cRNA samples were hybridized to a custom Illumina Sentrix Array Matrix (SAM; Illumina Inc., San Diego, CA) for 16～18 h at 55℃, following the manufacturer's instructions. The SAM contains 96 identical oligonucleotide arrays, consisting of 710 genes, 698 user-selected and housekeeping genes, and 12 negative control sequences. There were two 50-mer probes representing each gene. The SAM was washed, blocked with casein in phosphate buffered saline (PBS), incubated with streptavidin-Cy3, dried, and scanned on an Illumina® BeadArray Reader GX.

4 Reverse transcription and quantitative real-time PCR

Total RNA was reverse transcribed in a final volume of 20 μL using 1 μg of total RNA, 1 μL oligo-dT primers, and 25 mM dNTP. After samples were heated for 5 min at 65 C, 4 μL of 5× First-strand buffer, 1 μL dithiothreitol, and 1 μL of Superscript II RNase H-reverse transcriptase (Invitrogen) were added. Reverse transcription was performed at 37℃ for 50 min. The cDNA was stored at −20℃. Quantitative real-time PCR (qPCR) was performed using the primers shown in Table 1. qPCR was done using an Mx3000P (Stratagene, Austin, TX) using the SYBR Premix Ex Taq (Perfect Real Time) master mixture (Takara, Japan). Each reaction mixture contained 2 μL of template cDNA, a final concentration of 0.2 μM of forward and reverse primers, 10 μL of 2× SYBR Premix Ex Taq, 0.4 μL of 50× ROX Dye II, and RNase-free dH_2O to make a final volume of 20 μL. PCR for each gene consisted of the following sequence: 95℃, 10 sec for initial denaturation, and 40 cycles of 95℃ for 5 sec and 60℃ for 20 sec. To determine primer specificity, three stages (95℃ for 15 s, 60℃

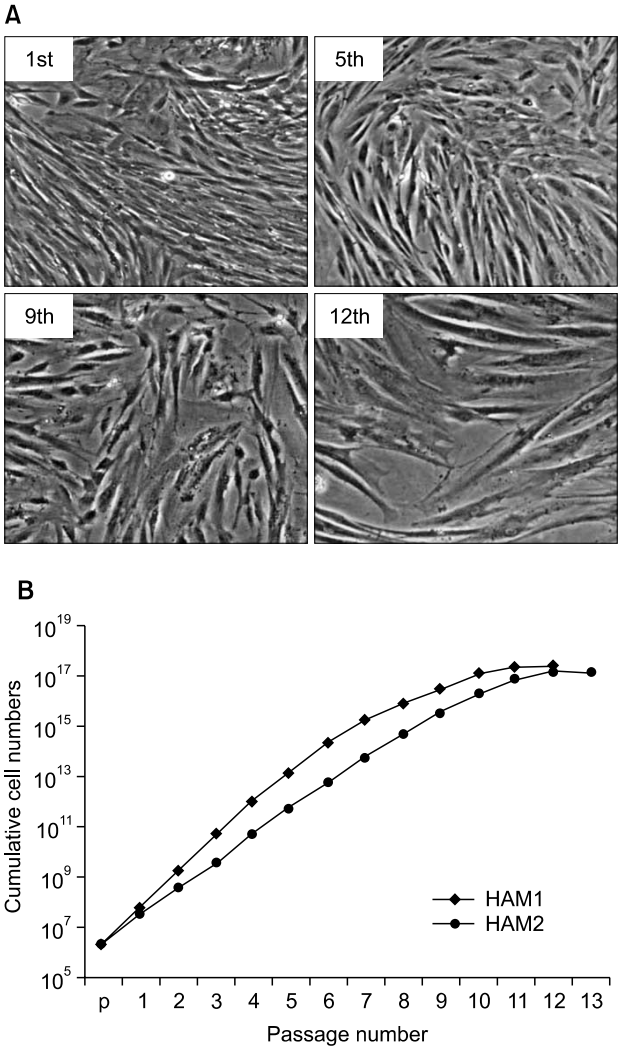

Fig. 1. Morphology of HAF stem cells and cumulative cell numbers with passage numbers. (A) Phase contrast pictures of HAF stem cells as a function of passage number (1st, 5th, 9th, and 12th): 40× magnification. (B) Cumulative cell growth curves for HAF stem cells until the 13th passage. HAF stem cells separated from two different pregnant women were independently counted and denoted as HAM1 and HAM2, respectively.

for 20 s, and 95℃ for 15 s, with a ramping time of 20 min) were added at the end of the PCR to obtain dissociation curves for each gene. qPCR data were analyzed by MxPro™ software (Stratagene). Relative transcript levels were determined using the $2^{-\triangle\triangle Ct}$ method and normalized to GAPDH.

Results

1 Senescence of stem cells derived from human amniotic fluid (HAF)

HAF stem cells were cultured as previously described (10). Average doubling time was approximately 3.6 days. By the 10th passage they stopped proliferating at which time their morphology was flat and large, which is one of the characteristics of cellular senescence after about 10 passages. This is distinct from the morphology of early-staged HAF stem cells (Fig. 1A). Consistent with the morphological changes, the cumulative cell number was not increased after 11 passages (Fig. 1B).

2 Gene expression profile of HAF stem cells according to passage numbers

To identify cellular senescence-associated genes, we performed illumina microarray chip assays using HAF stem cells at each passage (1st, 2nd, 4th, 6th, 8th, and 10th). Differentially expressed genes were grouped according to their expression profiles along the time course (Fig. 2). Of the 25,804 genes on the chip, 1970 showed an over 2-fold change relative to control (1st passage). Each of the 1970 genes was assigned to one of 9 distinct temporal expression clusters (Fig. 2B and C). Each cluster included genes showing expression profiles similar to each other, but distinct from genes in other clusters. In this analysis, a variety of expression patterns were identified, including ones that depicted gradually increasing expression levels (cluster 1, 3, and 5), and others that depicted early peaks of expression followed by decreasing expression levels (cluster 2, 4, 6, and 9) (Fig. 2C). Table 2 shows lists of gradually changed genes assigned to each cluster.

3 Expression patterns of aging-related genes during the process of senescence of HAF cells

To see the expression pattern of known aging-related genes such as

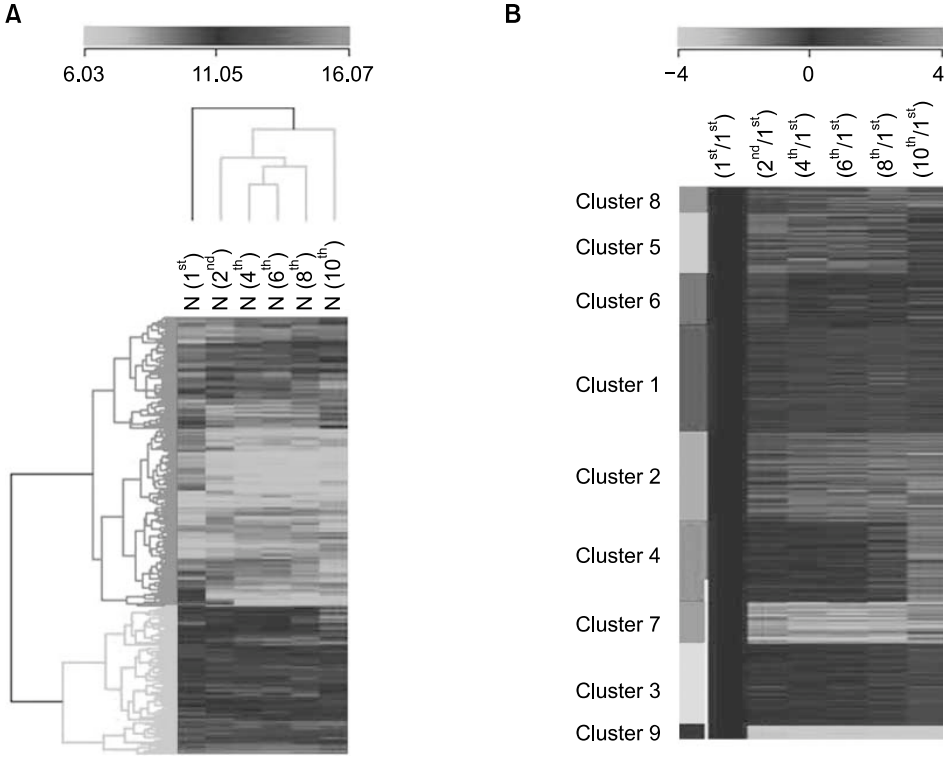

Fig. 2. Time course for gene expression analysis of HAF stem cells. (A) Hierarchical clustering of 1970 genes that showed over a 2-fold change in any later passages compared with the control group (1st passage) by a Euclidean method and complete linkage. Green and red colors indicate downregulated and upregulated expression, respectively. (B, C) k- means clusters of gene expression levels. Relative transcript level changes over time for individual genes in each cluster are displayed in graphical form in (C).

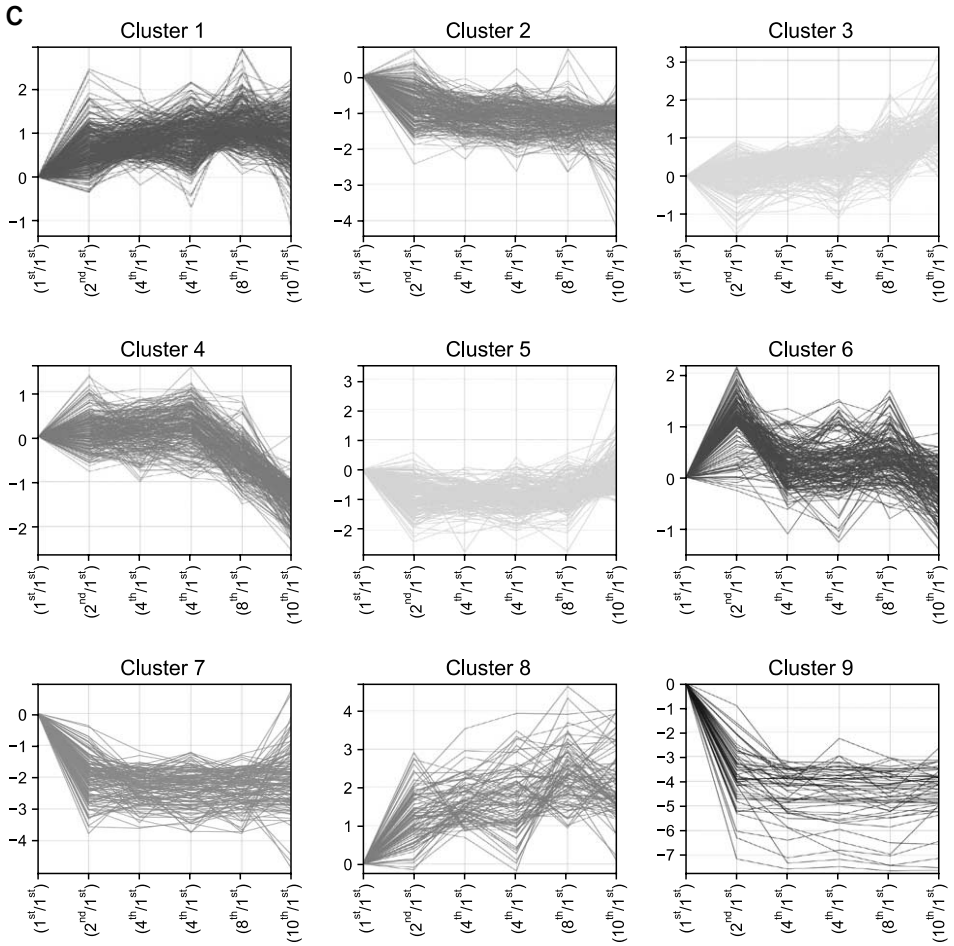

Fig. 2. Continued.

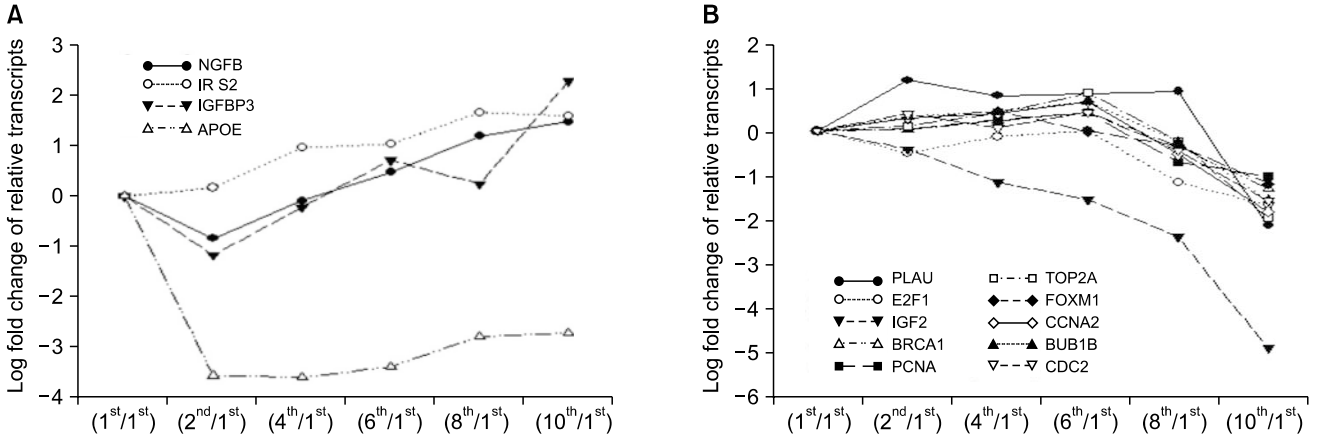

Fig. 3. Aging-related genes that showed time-dependent changes in expression patterns during the senescence of HAF stem cells. (A) Gradually upregulated genes. (B) Gradually downregulated genes.

p53, pRb, Bmi-1 during senescence of HAF cells, we analyzed chip data. Thirty eight aging-related genes were included among the 1,970 genes that showed over a 2-fold change relative to control. Contrary to our expectations, expression patterns of aging-related genes over time (i.e., over several passages) were mostly irregular although there were, rarely, big fold changes (data not shown). Among 38 genes, we

selected ones with gradually increasing or decreasing expression patterns (Fig. 3). Upregulated genes included nerve growth factor beta (NGFB), insulin receptor substrate 2 (IRS2), insulin-like growth factor binding protein 3 (IGFBP3), and apolipoprotein E (APOE). Expression of ten genes, including PLAU, E2F1, IGF2, BRCA1, TOP2A, PCNA, FOXM1, CCNA2, BUB1B, and CDC2, was gradually downregulated. In particular, IGF2 was drastically downregulated by the 10th passage.

4 Verification of the illumina chip data

To verify the illumina chip data, we selected several genes in Table 2 and examined their expression levels by quantitative real-time PCR (RT-qPCR) (Fig. 4). We selected eight genes (three upregulated genes and five downregulated genes) that were gradually and dramatically changed as a function of their passage number. These were receptors, signaling molecules, or cytoskeletal proteins. While folate receptor 3 (FOLR3), cadherin 6 (CDH6), and chemokine (C-X-C motif) ligand 12 (CXCL12) were upregulated, natriuretic peptide precursor B (NPPB), cyclin D2, insulin-like growth factor 2 (IGF2), keratin 8 (KRT8), and cellular retinoic acid binding protein 2 (CRABP2) were downregulated according to the chip data (Table 2). To confirm the chip data, RT-qPCR was performed. The expression pattern for both FOLR3 and CDH6 were gradually increased with passage number, consistent with the chip data. CXCL12 showed a drastic increase at the 4th passage and then decrease at the 10th passage even though the expression level was higher than that at the 1st passage. This was inconsistent with the chip data. Expression patterns of KTR8, NPPB, and CRABP2 were consistent with those of the chip data. However, the expression pattern of the IGF2 gene was different from the chip data. While IGF2 mRNA expression had decreased slightly by the 8th passage and then abruptly dropped in the chip data, RT-qPCR results indicated that gene expression had increased until the 6th passage and then was drastically downregulated. Very interestingly, a much more abrupt decrease in NPPB mRNA expression was shown by RT-qPCR than by the chip data.

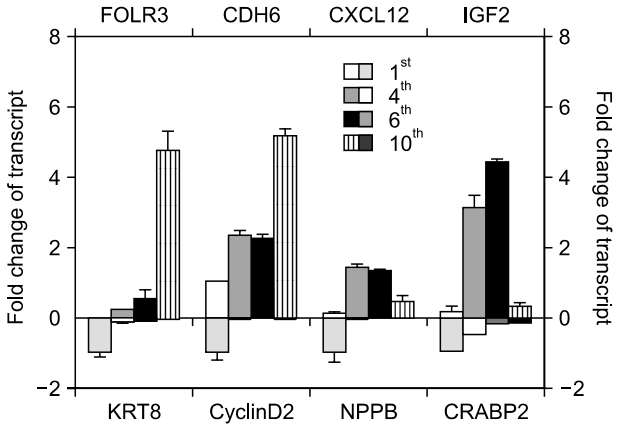

Fig. 4. Verification of illumina microarray data using RT-qPCR. RT-qPCR analysis of FOLR3, CDH6, KRT8, Cyclin D2, NPPB, CXCL12, CRABP2 and IGF2 were performed using HAF stem cells from the 1st, 4th, 6th, and 10th passages. GAPDH served as an internal control and was used for the normalization of each gene in qPCR. For relative mRNA expression, the value for the control group was defined as "0.01" for FOLR3 and "0.1" for CXCL12 and IGF2. For the expression of other genes, the value for the control group was defined as "1.0".

Discussion

Cellular senescence is considered to be one of the safeguard mechanisms against development of cancers. Therefore, an understanding of the genes controlling stem cell senescence may provide (i) relevant information on the mechanisms underlying malignant transformation of stem cells and (ii) therapeutic targets for novel anti-cancer agents. In this report, we did illumina microarray chip assays on HAF stem cells to find new senescence-related genes. We selected eight genes that had gradually and dramatically changed expression patterns and confirmed changes in expression levels by RT-qPCR. Our results strongly suggest that FOLR3 and NPPB are potent regulators that induce or suppress, stem cell senescence.

Environmental and hyperproliferative stressors can be potent inducers of senescence. The main two pathways involved in stress-induced senescence are p19-p53 and p16-Rb (11). Recently, it has been shown that the Bmi-1 oncogene functions as an inhibitor of senescence, while the overexpression of Bmi-1 extends the replicative lifespan. Bmi-1-null fibroblasts enter premature senescence through the p16-Rb pathway by p16 up-regulation (12). Also, it has been reported that Bmi-1 functions in vivo to maintain the pool of neuronal and hematopoietic stem cells by inhibiting their senescence program through the repression of p16 expression (13). Contrary to expectations, our chip data did not show any changes in the mRNA expression of these main senescence-regulated genes. However, this might be explained by the fact that since posttranslational protein modifications including phosphorylation, acetylation, and ubiqitination play important roles in both the activation and function of p53 and pRb (14), all mRNA level changes in these molecules cannot represent changes in their functions as transcriptional repressors inducing stem cell senescence. Alternatively, apart from the function of p53 and pRb, a senescence-associated cell cycle arrest can be induced by the downstream regulators of p53 and pRb such as a reduction in total E2F/DP activity (15). In addition, the downregulation of selected positive-acting cell cycle regulatory genes can also induce stem cell senescence, including the c-fos proto-oncogene, genes for Cdc2 and cyclin A and E, components of cyclin-dependent protein kinases (Cdks), genes for Id1 and Id2 inhibitors of basic helix-loop-helix transcription factors, and the multifunctional transcription factor E2F1 (16). Consistent with these previous results, our chip data also showed that gene expression of E2F1, cyclin A2 (CCNA2), and CDC2 were significantly down-

Table 2. Genes that gradually increased or decreased

Gene symbol	Accession no.	Fold change				
		2nd/1st	4th/1st	6th/1st	8th/1st	10th/1st
Cluster 1						
TSPAN10	NM_031945.2	1.25	1.77	2.39	2.63	4.51
DMPK	NM_0044092.2	1.60	1.95	1.51	1.92	3.85
CA5B	NM_007220.2	1.28	2.00	1.96	2.78	3.05
ALDH1A1	NM_000689.3	3.46	3.35	2.27	6.42	–2.47
BDNF	NM_001709.3	1.53	2.17	2.30	2.78	4.00
Cluster 2						
RGC32	NM_014059.1	–1.87	–2.19	–2.48	–1.90	–20.50
RNF144	NM_014746.2	–1.33	–2.16	–3.60	–3.34	–5.69
STRA6	NM_022369.2	1.32	–2.15	–3.76	–2.29	–4.83
EMILIN2	NM_032048.2	–1.33	–1.72	–1.92	–2.29	–4.83
NNAT	NM_005386.2	–1.21	–2.12	–2.17	–2.80	–4.22
CRABP2	**NM-001878.2**	**1.20**	**–1.53**	**–3.57**	**–2.39**	**–12.63**
CXCL5	NM_002994.3	–1.55	–1.75	–2.06	–2.86	–4.94
ISLR	NM_005545.3	–1.20	–1.67	–2.25	–2.19	–5.02
NDN	NM_002487.2	–1.29	–1.62	–2.72	–3.71	–6.97
F2RL1	NM_005242.3	–1.00	–3.27	–2.88	–3.47	–6.59
TSC22D1	NM_006022.2	1.68	–2.26	–1.96	–1.84	–3.66
SCARA3	NM_016240.2	–1.65	–1.31	–1.32	–2.23	–8.17
COL16A1	NM_001856.2	–1.01	–1.80	–1.79	–2.01	–4.00
TMEM119	NM_181724.1	–1.83	–2.21	–2.99	–2.05	–16.65
LRRC17	NM_001031692.1	1.18	–2.06	–1.27	–3.20	–7.52
CTHRC1	NM_138455.2	–1.19	–2.03	–1.76	–1.92	–5.22
DENND2A	NM_015689.2	–1.73	–1.18	–1.64	–1.52	–10.59
HMGB3	NM_005342.2	–1.21	–1.43	–1.66	–2.14	–2.91
Cluster 3						
IFNB1	NM_002176.2	–1.06	1.17	1.15	2.12	1.17
COL4A2	NM_001846.1	1.14	–1.53	–1.15	–1.30	2.01
MBP	NM_001025100.1	–2.21	–1.19	–1.24	2.20	1.23
SYVN1	NM_032431.2	–1.02	–1.03	1.17	2.02	1.01
GAS6	NM_000820.1	–1.26	1.07	1.44	1.59	2.69
IDUA	NM_000203.2	–1.01	–1.06	1.12	1.21	2.40
LPHN2	NM_012302.2	1.32	1.60	1.57	1.05	3.53
DCTN1	NM_023019.1	–1.16	1.35	1.17	1.38	2.18
CLEC3B	NM_003278.1	1.06	1.37	1.74	1.58	3.75
NCALD	NM_032041.1	1.01	1.54	1.47	1.23	3.39
TPST2	NM_001008566.1	–1.01	1.05	1.49	1.20	2.43
COL4A5	NM_033381.1	–1.47	–1.36	1.28	1.01	2.06
SORBS1	NM_015385.1	–1.14	–1.14	–1.42	–1.28	4.02
LATS2	NM_014572.1	–1.14	1.34	1.15	1.35	2.72
NGFB	NM_002506.2	–1.79	–1.07	1.39	2.29	2.79
PIGZ	NM_025163.2	–1.20	1.17	1.24	1.09	2.73
CAMK2D	NM_001221.2	–1.08	1.41	1.43	1.97	2.06
FBXO32	NM_058229.2	1.09	1.87	–1.03	3.77	6.68
SYNGR1	NM_145731.2	–1.01	1.75	2.00	2.15	5.07
PSG5	NM_002781.2	–2.84	1.02	2.00	2.18	3.51
DYSF	NM_003494.2	–1.39	1.37	1.64	1.58	9.91
IGFBP3	NM_001013398.1	–2.25	–1.16	1.64	1.18	4.89
HIST2H2BE	NM_003528.2	–1.42	1.06	1.10	1.62	3.31
ST3GAL6	NM_006100.2	–1.43	1.29	1.33	1.99	2.31

Table 2. Continued

Gene symbol	Accession no.	Fold change				
		$2^{nd}/1^{st}$	$4^{th}/1^{st}$	$6^{th}/1^{st}$	$8^{th}/1^{st}$	$10^{th}/1^{st}$
CNN1	NM_001299.4	–1.03	–141.00	–1.58	–1.47	2.81
SLC20A2	NM_006749.3	–1.02	1.43	1.43	2.06	3.18
NTN4	NM_021229.2	–1.41	1.59	1.58	2.66	3.41
FBXO32	NM_148177.1	–1.41	1.28	–1.50	2.49	3.86
SYNPO4	XM_942780.1	–1.01	1.30	1.28	1.58	6.47
PSG6	NM_001031850.1	–2.60	–1.28	1.31	1.25	2.66
CCPG1	NM_004748.3	–1.02	–1.04	1.12	1.74	2.87
MCOLN1	NM_020533.1	–1.04	1.04	1.10	1.56	2.02
CYP2U1	NM_183075.2	–1.28	1.50	2.17	2.19	3.51
CDH6	**NM_004932.2**	**1.53**	**1.38**	**1.77**	**1.42**	**6.81**
Cluster 4						
Cyclin B1	NM_031966.2	1.02	1.51	1.54	–1.06	–2.75
ATAD2	NM_014109.2	1.37	1.23	1.55	–1.74	–3.11
SPAG5	NM_006461.3	1.32	1.36	1.43	–1.35	–3.03
POLQ	NM_199420.2	1.28	1.37	1.66	–1.25	–3.04
E2F1	NM_005225.1	–1.42	–1.10	–1.0	–2.27	–3.24
KIF4A	NM_012310.2	1.23	1.33	1.43	–1.06	–2.42
PTTG1	NM_004219.2	2.49	1.46	1.32	1.03	–3.63
CKS1B	NM_001826.1	1.26	1.02	–1.04	–1.38	–3.26
FKSG14	NM_022145.2	1.21	1.08	1.28	–1.45	–2.55
MCM7	NM_182776.1	1.14	1.11	–1.05	–2.27	–4.39
SIPA1L2	NM_0208081.1	1.60	–1.24	–1.92	–1.31	–2.72
CDC2	NM_033379.2	1.34	1.19	1.62	–1.44	–4.79
KIF23	NM_004856.4	1.12	1.14	1.33	–1.56	–2.78
FANCD2	NM_001018115.1	1.12	1.36	1.45	–1.12	–2.10
UHRF1	NM_016195.2	1.31	1.36	1.72	–1.08	–2.90
MPHOSPH1	NM_016195.2	1.31	1.36	1.72	–1.08	–2.90
MGC39900	NM_194324.1	2.09	1.01	–1.04	–1.48	–2.10
STK6	NM_198434.1	1.11	1.31	1.70	–1.32	–3.14
MMP3	MN_002422.3	–1.29	–1.52	–1.25	–1.65	–5.21
ACAT2	NM_005891.1	1.01	1.04	–1.29	–1.81	–2.85
TROAP	NM_005480.2	1.30	1.48	1.47	–1.24	–3.14
SALL2	NM_005407.1	1.21	–1.05	–1.60	–1.62	–2.26
DTYMK	NM_012145.2	1.94	1.04	–1.00	–1.55	–2.51
MELK	NM_014791.2	1.26	1.09	1.29	–1.43	–3.02
KNTC2	NM_006101.1	1.03	1.33	1.81	–1.25	–3.59
KIF20A	NM_005733.1	1.87	2.08	2.04	1.18	–2.59
NUSAP1	NM_016359.2	1.32	1.50	1.53	–1.13	–3.67
TRIP13	NM_004237.2	1.04	1.26	1.15	–1.40	–3.55
Cyclin B2	NM_004701.2	1.16	1.35	1.38	–1.38	–4.26
Cyclin A2	NM_001237.2	1.23	1.32	1.59	–1.45	–3.58
CDCA1	NM_031423.2	1.01	1.29	1.67	–1.15	–2.60
HMMR	NM_012485.1	1.70	1.43	2.16	–1.02	–3.38
DNMT1	NM_001379.1	1.31	1.14	1.25	–1.41	–2.39
FAM64A	NM_019013.1	1.39	1.54	1.36	–1.38	–3.61
CDCA3	NM_031299.3	1.23	1.76	1.87	–1.34	–2.72
CDT1	NM_030928.2	1.03	1.02	1.09	–2.49	–5.00
E2F2	NM_004091.2	1.40	1.24	1.27	–2.19	–4.15
EXOSC8	NM_181503.1	1.06	–1.01	–1.10	–1.31	–2.59
CREB5	NM_001011666.1	1.29	–1.32	–1.05	–1.52	–2.31

Table 2. Continued

Gene symbol	Accession no.	Fold change				
		2nd/1st	4th/1st	6th/1st	8th/1st	10th/1st
TOP2A	NM_001067.2	1.08	1.32	1.81	–1.18	–3.97
CYB5R2	NM_016229.2	–1.04	–1.17	–1.29	–1.08	–3.97
MCM5	NM_006739.2	1.01	1.22	–1.06	–2.16	–3.31
TPX2	NM_012112.4	1.04	1.54	1.50	–1.06	–2.58
PRC1	NM_003981.2	1.60	1.70	1.61	–1.11	–2.86
ROR2	NM_004560.2	–1.27	–1.54	–1.55	–1.15	–3.21
ZWINT	NM_032997.2	1.22	1.08	1.16	–1.77	–2.75
GLDC	NM_000170.1	1.42	–1.68	–1.69	–1.89	–3.26
H2AFX	NM_002105.2	1.10	1.34	1.25	–1.68	–2.82
HCAP-G	NM_022346.3	1.08	1.43	1.66	–1.26	–3.87
FANCG	NM_004629.1	1.02	1.10	1.19	–1.42	–2.39
MAD2L1	NM_002358.2	1.41	1.18	1.57	–1.55	–3.54
PLAU	NM_002658.2	2.21	1.74	1.79	1.86	–4.48
CDC2	NM_001786.2	1.30	1.05	1.35	–1.37	–3.03
MCM10	NM_018518.3	1.08	1.03	1.21	–2.06	–3.73
RAD51AP1	NM_006479.2	1.32	1.58	1.88	1.02	–2.93
RANBP1	NM_002882.2	2.18	–1.00	–1.16	–1.23	–2.83
KNTC1	NM_014708.3	1.16	1.23	1.27	–1.28	–2.83
KIF2C	NM_006845.2	1.08	1.16	1.39	–1.30	–4.41
PFS2	NM_016095.1	1.02	1.11	1.10	–2.53	–4.30
CTF18	NM_022092.1	1.33	1.22	1.14	–1.27	–2.32
KIF14	NM_014875.1	1.37	1.10	1.63	–1.12	–2.71
TK1	NM_003258.1	1.05	1.35	1.18	–1.54	–2.59
CDCA5	NM_080668.2	1.10	1.30	1.32	–1.31	–3.90
HMGB5	NM_002129.2	1.46	1.53	1.64	1.13	–2.39
MCM4	NM_005914.2	1.71	1.05	1.17	–1.57	–3.28
PBK	NM_018492.2	1.07	1.18	1.60	–1.51	–4.45
HNRPH1	NM_005520.1	2.05	1.18	–1.02	–1.24	–2.28
DLG7	NM_014750.3	1.33	1.60	1.87	–1.06	–3.65
CENPA	NM_001809.2	1.54	1.33	1.57	1.02	–4.08
SCARA3	NM_182826.1	–1.58	–1.17	–1.19	–2.05	–4.27
KIF15	NM_020242.1	1.02	1.28	1.41	–1.23	–3.02
UBE2C	NM_181803.1	1.35	1.28	1.41	–1.13	–5.14
KRT19	NM_002276.3	–1.00	–1.09	–1.38	–1.56	–4.20
SGOL2	NM_152524.3	1.15	1.35	1.61	–1.10	–2.11
CENPE	NM_001813.2	1.52	1.35	1.99	–1.08	–3.04
CDC20	NM_001255.1	1.13	1.36	1.32	–1.47	–4.79
KIF11	NM_004523.2	1.02	1.39	1.69	–1.31	–3.08
SPBC25	NM_020675.3	1.08	1.24	1.54	–1.46	–3.04
UBE2T	NM_014176.1	1.52	1.23	1.33	–1.25	–3.02
FBX5	NM_012177.2	1.32	1.16	1.50	–1.42	–3.44
Cluster 5						
GCLC	NM_001498.2	–2.03	–1.50	–1.31	1.39	1.03
TUFT1	NM_020127.1	–3.46	–2.41	–2.83	–2.06	1.02
COBLL1	NM_014900.3	–4.65	–2.52	–2.38	–1.49	–1.62
TSRC1	NM_025008.2	–3.35	–1.92	–1.28	–1.29	1.24
RASGRP1	NM_005739.2	–2.75	–1.83	–1.98	–1.50	1.21
FUCA1	NM_000147.2	–2.46	–2.63	–2.22	–1.72	1.15
CAST	NM_173060.1	–2.48	–1.31	–1.28	–1.46	1.00
PSG11	NM_002785.2	–3.61	–2.08	1.06	–1.15	1.31
FKHL18	NM_004118.3	–1.69	–2.40	–3.74	–3.84	1.27

Table 2. Continued

Gene symbol	Accession no.	Fold change				
		$2^{nd}/1^{st}$	$4^{th}/1^{st}$	$6^{th}/1^{st}$	$8^{th}/1^{st}$	$10^{th}/1^{st}$
PSG9	NM_002784.2	–2.91	–1.65	1.17	–1.23	1.32
HES4	NM_021170.2	–2.63	–2.20	–2.73	1.01	1.02
NTF3	NM_002527.3	–1.38	–2.38	–2.49	–.32	2.05
CTPS	NM_001905.1	–2.16	–1.86	–1.67	–1.99	1.14
ACTC (Actin alpha)	NM_005159.3	–5.21	–3.41	1.33	–2.63	10.73
IMPA2	NM_014214.1	–2.94	–1.64	–1.89	–1.31	1.37
CLIC3	NM_004669.2	–3.78	–1.57	–3.24	–1.61	1.30
PPP1R14A	NM_033256.1	–1.40	–2.15	–3.61	–2.43	3.22
PRSS23	NM_007173.3	–1.76	–1.49	–1.12	–1.40	2.26
HSPB2	NM_001541.2	–3.46	–2.81	–2.43	–2.24	1.66
AK3L1	NM_001005353.1	–3.50	–3.21	–3.97	–2.98	1.81
Cluster 6						
HSD11B1	NM_005525.2	2.53	1.26	1.36	1.51	–1.24
LXN	NM_020169.2	1.98	1.12	–1.06	–1.11	–2.01
CASP1	NM_033294.2	2.86	2.12	1.60	2.86	–1.24
PHLDA1	NM_007350.2	1.86	1.29	1.25	1.47	–2.06
HOXA5	NM_019102.2	2.41	1.57	1.36	1.26	–1.35
MT1X	NM_005952.2	3.59	1.73	1.55	1.82	–1.37
TFP12	NM_006528.2	2.26	2.09	2.74	2.25	–2.04
BDKRB1	NM_000710.2	1.32	1.47	2.23	1.48	–2.09
CACYBP	NM_014412.2	2.80	1.02	1.22	–1.09	–1.82
SSFA2	NM_006751.3	4.09	1.41	1.39	1.35	–1.02
SNX5	NM_152227.1	3.39	1.07	1.20	1.07	–1.55
Cluster 7						
PDPN	NM_001006625.1	–2.94	–4.77	–11.09	–7.46	–26.46
CYP1B1	NM_000104.2	–3.05	–9.59	–8.07	–6.24	–11.76
OLR1	NM_002543.2	–9.96	–4.12	–3.38	–4.34	–2.27
IGF2	**NM_000612.2**	**–1.33**	**–2.25**	**–2.98**	**–5.35**	**–30.83**
WFDC1	NM_021197.2	–8.02	–11.84	–10.89	–13.68	1.03
MAMDC2	NM_153267.3	–9.16	–7.37	–7.33	–5.73	–4.21
CRYAB	NM_001885.1	–7.24	–5.09	–4.43	–3.81	1.64
GFPT2	NM_005110.1	–1.30	–3.91	–4.54	–6.86	–22.61
Cluster 8						
IFIT1	NM_001548.2	3.74	5.06	5.33	10.47	9.44
NEFL	NM_006158.1	3.14	3.90	5.57	4.78	12.58
SGIP1	NM_032291.1	2.48	3.69	3.35	5.90	6.20
FOLR3	**NM_000804.2**	**1.07**	**2.97**	**3.51**	**5.88**	**12.38**
RAB33A	NM_004794.2	1.38	2.88	1.81	4.90	8.95
LCE2A	NM_178428.3	1.58	2.72	9.57	8.24	15.82
LAMA4	NM_002290.2	3.24	4.15	4.82	4.91	8.01
CXCL12	**NM_199168.2**	**2.43**	**4.71**	**5.79**	**3.68**	**17.19**
OSAP	NM_032623.2	4.23	11.55	15.27	15.05	16.30
Cluster 9						
KRT7	**NM_005556.3**	**–18.05**	**–18.60**	**–16.58**	**–26.81**	**–26.12**
NPPB	**NM_002512.1**	**–16.40**	**–59.05**	**–88.10**	**–125.19**	**–28.97**
EPB41L3	NM_012307.2	–7.15	–9.12	–12.29	–20.57	–31.32
Cyclin D2 (CCND2)	**NM_001759.2**	**–3.10**	**–10.40**	**–27.54**	**–24.49**	**–17.23**
H19	NR_002196.1	–39.75	–59.62	–121.63	–172.19	–183.23
AQP1	NM_198098.1	–17.74	–161.22	–144.80	–172.35	–138.12
MMP10	NM_002425.1	–1.90	–12.17	–10.29	–12.83	–21.22
KRT8	NM_002273.2	–8.45	–38.53	–52.00	–58.27	–40.68

Table 3. Genes related to aging with an over 2-fold change

Gene symbol	Accession no.	Fold change				
		2nd/1st	4th/1st	6th/1st	8th/1st	10th/1st
GHR	NM_000163	**–2.09**	–1.78	–1.68	**–2.02**	–1.49
TERC	NR_001566	1.54	1.92	**2.41**	1.97	1.01
PLAU	NM_002658	**2.21**	1.74	1.79	1.86	**–4.48**
E2F1	NM_005225	–1.42	–1.10	–1.00	**–2.27**	**–3.24**
NRG1	NM_013959	–1.17	–1.18	1.29	–1.23	2.11
IGF2	NM_000612	–1.33	**–2.25**	**–2.98**	**–5.35**	**–30.83**
NGFB	NM_002506	–1.79	–1.07	1.39	2.29	2.79
IRS2	NM_003749	1.12	1.95	**2.06**	**3.18**	**3.02**
EGF	NM_001963	1.02	1.43	1.71	1.18	**2.67**
FOS	NM_005252	–1.04	–2.01	–2.07	–1.75	**–3.21**
PARP1	NM_001618	–1.06	1.11	–1.03	–1.35	**–2.14**
BRCA1	NM_007294	1.02	1.17	1.33	–1.29	**–2.50**
BLM	NM_000057	–1.18	1.18	1.13	–1.46	**–2.05**
IGFBP3	NM_000598	–2.25	–1.16	1.64	1.18	**4.89**
TOP2A	NM_001067	1.08	1.32	1.81	–1.18	**–3.97**
RAD51	NM_002875	–1.10	–1.04	1.02	–1.74	**–2.11**
PRKCA	NM_002737	–1.13	1.58	**2.08**	1.67	1.51
RFC4	NM_181573	–1.03	1.07	1.07	–1.89	**–2.90**
PCNA	NM_182649	1.03	1.19	1.34	–1.64	**–2.06**
FEN1	NM_004111	1.50	–1.09	1.08	**–2.01**	**–2.72**
FOXO1A	NM_002015	–1.91	**–2.42**	**–4.80**	**–3.54**	**–2.69**
SOD2	NM_000636	1.67	**2.46**	1.24	**2.50**	1.50
FOXM1	NM_021953	1.22	1.37	–1.01	–1.27	**–2.30**
APOE	NM_021953	**–11.82**	**–12.19**	**–10.48**	**–6.92**	**–6.60**
IL6	NM_000600	1.19	**2.22**	1.03	2.90	1.33
CCNA2	NM_001237	1.23	1.32	1.59	–1.45	**–3.58**
HMGB2	NM_002129	1.46	1.53	1.64	1.13	**–2.39**
MAP3K5	NM_005923	1.98	**2.54**	1.93	2.72	1.44
MLLT7	NM_005938	**–6.21**	**–7.30**	**–7.34**	**–6.56**	**–3.85**
TFAP2A	NM_003220	1.98	**4.60**	**5.48**	**4.00**	**3.26**
BUB1B	NM_001211	1.26	1.35	1.58	–1.20	**–2.99**
PTGS2	NM_000963	–1.30	–1.26	–1.46	1.57	**–3.29**
CDC2	NM_001786	1.30	1.05	1.35	–1.37	**–3.03**
DDIT3	NM_004083	1.89	1.61	–1.13	**11.13**	**2.63**
H2AFX	NM_002105	1.10	1.34	1.25	–1.68	**–2.82**
NFKBIA	NM_020529	–1.18	–1.46	**–2.22**	–1.90	**–2.74**
GCLC	NM_001498	**–2.03**	–1.50	–1.31	1.39	1.03
GCLM	NM_002061	–1.13	–1.61	–1.10	–1.34	**–2.01**

regulated at the latter passage numbers (8th and 10th passages) (Table 3) although we didn't verify the expression pattern of these genes by RT-PCR or RT-qPCR in this study.

Here we selected eight genes including FOLR3, CDH6, CXCL12, NPPB, cyclin D2, IGF2, KRT8, and CRABP2, for verifying results from the chip data because these genes showed gradual and drastic changes in expression patterns. It has not been reported to date that these selected genes are directly related to cellular senescence. Although an interest in IGF2 derives mostly from its connection with IGF1 and how the IGF1/GH axis appears to regulate aging in model organisms, IGF2's role in aging is unproven (17). Recently, it was reported that overall IGF2 expression increased during senescence of human prostate epithelial cells due to the loss of IGF2 imprinting (18). However, our RT-qPCR result, which did not match our chip data, showed that IGF2 mRNA levels were increased by the 6th passage and then abruptly dropped by the 10th passage (Fig. 4). The discrepancy between our result and theirs might be caused by our using different cell types. Or, IGF2 might not be a main regulator of cellular senescence. The cellular retinoic acid binding proteins (CRABPs) are cytoplasmic receptor proteins for retinoic acid, which has been used as a therapeutic drug since it induces the senescence of tumor cells (19). These proteins play a role in the binding, transport, and metabolism of retinoic acid. Growth inhibition and apoptosis in retinoid-treated MCF-7 cells have been previously associated with the retinoid-binding protein CRABP2 (20). Although HAF stem cells were not treated with retinoids in this study, we also found that CRABP2 was strongly downregulated with increases in passage number (Fig. 4). These results suggest that CRABP2 might potentially act as a negative regulatory mechanism that limits cellular senescence. Unexpectedly, mRNA levels of both NPPB and FOLR3 were dramatically downregulated and upregulated, respectively, in both our chip data and in our qRT-PCR. Although it has been reported that the level of NPPB is particularly important in heart disease, since increased levels of this peptide in the circulation is a clinical indicator of the severity of hypertrophy (21), there has not yet been a published study about the role of NPPB in cellular senescence. Folate metabolism and its receptors have been reported to be related to cancer development, especially, cancers that originate from epithelial cells (22). Animal experiments suggest that proper supplementation with folate can reduce carcinogenesis, whereas excessive supplementation may increase tumor growth (23). These opposing effects are thought to be attributable to an essential requirement for folate in the synthesis of DNA precursors needed to support rapidly proliferating tissues. Tumor cells frequently upregulate folate receptors (FOLR) to satisfy their elevated need for nucleotides to support DNA synthesis and growth (24). Furthermore, the high affinity of FOLRs, especially, FOLR1, for folate and its selective overexpression in tumors provides an opportunity for tumor-specific chemotherapy and radiopharmaceutical delivery, *e.g.*, folic acid analogues and conjugates, such as 5,10-dideazatetrahydrofolic acid, which are directly cytotoxic and therapeutically effective against some types of tumors. However, FOLR3 has not yet been reported to play an important role in cancer development and cellular senescence. Taken together, changed expression levels of NPPB and FOLR3 might be good markers for cellular senescence.

Conclusion

Future studies should be aimed at revealing whether NPPB or FOLR3 are directly involved in stem cell senescence and how they are regulated in response to replicative and stress-induced signals that cause stem cell senescence. Discovering the regulatory mechanisms of these genes should make it possible to design new therapeutic approaches to improving the efficacy and to decreasing the side effects of cancer therapy that target differentiated tumor cells as well as non-differentiated tumor stem cells.

References

1. Gosden CM. Amniotic fluid cell types and culture. Br Med Bull. 1983;39:348-54.
2. Milunsky A. Amniotic fluid cell culture. In: Milunsky A, editors. Genetic disorder and the fetus. New York: Plenum Press; 1979. p. 75-84.
3. Prusa AR, Marton E, Rosener M, Bernaschek G, Hengstschläger M. Oct-4 expressing cells in human amniotic fluid: a new source for stem cell research? Hum Reprod. 2003;18:1489-93.
4. Tsai MS, Lee JL, Chang YJ, Hwang SM. Isolation of human multipotent mesenchymal stem cells from second-trimester amniotic fluid using a novel two-stage culture protocol. Hum Reprod. 2004;19:1450-6.
5. Jacob J, Kieboom K, Marino S, DePinho RA, van Lohuizen M. The oncogene and polycomb-group gene bmi1 regulates cell proliferation and senescence through the ink4a locus. Nature. 1999;397:164-8.
6. Bauer JH, Poon PC, Glatt-Deeley H, Abrams JM, Helfand SL. Neuronal expression of p53 dominant-negative proteins in adult Drosophila melanogaster extends life span. Curr Biol. 2005;15:2063-8.
7. Tyner SD, Venkatachalam S, Choi J, Jones S, Ghebranious N, Igelmann H, et al. p53 mutant mice that display early ageing-associated phenotypes. Nature. 2002;415:45-53.
8. Noda A, Ning Y, Venable SF, Pereira-Smith OM, Smith JR. Cloning of senescent cell-derived inhibitors of DNA synthesis using an expression screen. Exp Cell Res.1994; 211:90-8.
9. Bond J, Jones C, Haughton M, DeMicco C, Kipling D, Wynford-Thomas D. Direct evidence from siRNA-directed "knock down" that p16 (INK4a) is required for human fibroblast senescence and for limiting ras-induced epithelial cell proliferation. Exp Cell Res. 2004;292:151-6.
10. Kim J, Lee Y, Kim H, Hwang KJ, Kwon HC, Kim SK, et al. Human amniotic fluid-derived stem cells have characteristics of multipotent stem cells. Cell Prolif. 2007; 40:75-90.
11. Pelicci PG. Do tumor-suppressive mechanisms contribute to organism aging by inducing stem cell senescence? J Clin Invest. 2004;113:4-7.
12. Itahana K, Zou Y, Itahana Y, Martinez JL, Beausejour C, Jacobs JJ, et al. Control of the replicative life span of human fibroblasts by p16 and the polycomb protein Bmi-1. Mol Cell Biol. 2003;23:389-401.
13. Park IK, Qian D, Kiel M, Becker MW, Pihalja M, Weissman IL, et al. Bmi-1 is required for maintenance of adult self-renewing haematopoietic stem cells. Nature. 2003;423:302-5.
14. Feng L, Lin T, Uranishi H, Gu W, Xu Y. Functional analysis of the roles of posttranslational modifications at the p53 C terminus in regulating p53 stability and activity. Mol Cell Biol. 2005;25:5389-95.
15. Maehara K, Yamakoshi K, Ohtani N, Kubo Y, Takahashi A, Arase S, et al. Reduction of

total E2F/DP activity induces senescence-like cell cycle arrest in cancer cells lacking functional pRb and p53. J Cell Biol. 2005;168:553-60.
16. Campisi J, Dimri GP, Hara E. Control of replicative senescence. In: Schneider E, Rowe J, editors. Handbook of the biology of aging. 4th ed. New York NY: Academic Press; 1996. p. 121-49.
17. Gil EB, Malone Link E, Liu LX, Johnson CD, Lees JA. Regulation of the insulin-like developmental pathway of Caenorhabditis elegans by a homolog of the PTEN tumor suppressor gene. Proc Natl Acad Sci U S A. 1999;96:2925-30.
18. Fu VX, Schwarze SR, Kenowski ML, Leblanc S, Svaren J, Jarrard DF. A loss of insulin-like growth factor-2 imprinting is modulated by CCCTC-binding factor down-regulation at senescence in human epithelial cells. J Biol Chem. 2004;279:52218-26.
19. Si SP, Tsou HC, Lee X, Peacocke M. Effect of cellular senescence and retinoic acid on the expression of cellular retinoic acid binding proteins in skin fibroblasts. Exp Cell Res. 1995;219:243-8.
20. Donato LJ, Noy N. Suppression of mammary carcinoma growth by retinoic acid: proapoptotic genes are targets for retinoic acid receptor and cellular retinoic acid-binding protein II signaling. Cancer Res. 2005;65:8193-9.
21. Burnett JC JR, Kao PC, Hu DC, Heser DW, Heublein D, Granger JP, et al. Atrial natriuretic peptide elevation in congestive heart failure in the human. Science. 1986;231:1145-7.
22. Kane MA, Portillo RM, Elwood PC, Antony AC, Kolhouse JF. The influence of extracellular folate concentration on methotrexate uptake by human KB cells. Partial characterization of a membrane-associated methotrexate binding protein. J Biol Chem. 1986;261:44-9.
23. Kim YI. Folate, colorectal carcinogenesis, and DNA methylation: lessons from animal studies. Environ Mol Mutagen. 2004;44:10-25.
24. Ross JF, Chaudhuri PK, Ratnam M. Differential regulation of folate receptor isoforms in normal and malignant tissues in vivo and in established cell lines. Physiologic and clinical implications. Cancer. 1994;73:2432-43.